Microelectronics Reliability 54 (2014) 404–409

Contents lists available at ScienceDirect

Microelectronics Reliability

journal homepage: www.elsevier.com/locate/microrel

Quantum coupling effects on charging dynamics of nanocrystalline memory devices

Ling-Feng Mao *

Institute of Intelligent Structure and System, School of Urban Rail Transportation, Soochow University, Suzhou 215006, PR China

ARTICLE INFO

Article history:
Received 20 June 2013
Received in revised form 13 October 2013
Accepted 14 October 2013
Available online 30 October 2013

ABSTRACT

A model is proposed to account for the impacts of the quantum coupling between the longitudinal and transverse components of the channel electron motion on the charging dynamics of memory devices. The calculations demonstrate that the quantum coupling effects on the charging dynamics of Ge NC (germanium nanocrystalline) memory devices cannot be neglected for high temperature and drift velocity of the channel electrons higher than the thermal velocity. The calculations also show that the charging current of Ge NC memory devices strongly depends on the temperature, drift velocity and effective electron mass of the tunneling oxide layer. The reduction in the barrier height caused by the quantum coupling is its origin. The sensitivity of the effective electron mass of the tunneling oxide layer on the charging current of Ge NC memory devices is a potential method to improve the performance of device.

1. Introduction

Conventional floating gate non-volatiles memories present critical issues for device scalability, such as gate length and tunnel oxide thickness reduction. Si and Ge NC quantum dot flash memories are fully complementary MOS (metal-oxide-semiconductor) compatible technology and have the potential of pushing the device scalability. Memory structures based on Ge NCs have received much attention for next-generation non-volatile memory devices due to their extended scalability and improved memory performance [1–7]. The characteristics of the Ge NCs produced by a dewetting process during annealing of an amorphous Ge layer deposited on an ultra thin SiO_2 layer as a function of the nominal Ge layer thickness has been investigated [1]. The Ge nanocrystal density and size effects on the carrier storage and emission processes have been studied [2]. Electron (hole) charge and discharge dynamics have been studied on plasma enhanced chemical vapor deposition grown metal-oxide-silicon Ge NC flash memory devices [3]. The electronic structure of Ge NC is studied using a sp^3 tight binding description [4]. Parameter-free calculations of the frequency-dependent dielectric function in order to understand the optical properties of Ge and Si NCs were presented [5]. Ge NCs embedded in amorphous silicon and self-organized on a tunnel silicon dioxide layer thermally grown on (100) *p*-doped silicon substrate have been electrically studied at different temperatures by using current–voltage and capacitance–voltage measurements [6]. The behaviors of charge trapping and charge retention in the Ge NC memory devices have been studied [7]. It is well-known that the crystal size of semiconductor less than 100 nm can lead to a larger band gap and a change in dielectric constant, thus the size of Ge NCs effects on the charging dynamics of memory devices has been studied [8]. Additionally, the quality of the grown Si/SiO_2 interface can significantly affects on the performance and reliability of a NC memory device, and thus the interface traps effects on the redetection time of Ge NC memory devices have been studied [9]. But in these work, the quantum coupling effects on tunneling current are neglected.

The tunneling current through an ultrathin oxide due to defect-mediated tunneling and quantum–mechanical direct tunneling give the main contribution to the charge and discharge dynamics of carriers in nanocrystal memories. Most studies on the tunneling currents imply the approximation that the components of electron motion in three directions are decoupled. In the previous work, a reduction in the barrier height caused by the quantum coupling between the longitudinal and transverse components of the thermal energy of tunneling electrons has been discussed on SiO_2, hafnium silicate, and HfO_2 gate dielectric [10–12]. The calculated Fowler–Nordheim tunneling currents with quantum coupling effects agree well with the experimental data [10,12]. Such quantum coupling effects result from the difference between the effective electron masses of the gate dielectrics and the gate (substrate). And it has also been demonstrated that neglecting quantum coupling effects result in a larger error in the estimation of the tunneling current and quantization of the inversion layer when the injection channel electron velocity in a MOSFET is higher than the thermal velocity 1×10^5 m/s [13,14]. The temperature-dependent experimental current data for SiO_2 agree very well with those calculated from the tunneling current model including quantum coupling effects [10]. The goal of the present paper is to theoreti-

* Tel.: +86 512 67501742; fax: +86 512 67601052.
E-mail address: lingfengmao@suda.edu.cn

0026-2714/$ - see front matter © 2013 Elsevier Ltd. All rights reserved.
http://dx.doi.org/10.1016/j.microrel.2013.10.015

cally depict a physical picture of the quantum coupling impacts on the charging dynamics of a Ge NC memory device and how it changes with temperature and the channel electron velocity.

2. Theory

Because the transverse momentum of the tunneling electron preserves conservation in the tunneling process, the Schrödinger equation in the gate oxide of a MOS structure can be written as [10–14]:

$$\left[-\frac{\hbar^2}{2m^*_{ox}}\frac{\partial^2}{\partial z^2}+\left(U(z)-\frac{\hbar^2k_r^2}{2m^*_{\perp-\mathrm{Si}}}\left(1-\frac{m^*_{\perp-\mathrm{Si}}}{m^*_{ox}}\right)\right)\right]\phi(z)=E_z^s\phi(z) \quad (1)$$

where $m^*_{\perp-\mathrm{Si}}$ are the transverse masses of electron in the substrate (gate) region, m^*_{ox} is the effective electron mass in the oxide (it is assumed to be direction-independent because the oxide is amorphous), $\hbar$ is the reduced Planck's constant, k_r is the wave vector of tunneling electron, $U(z)$ represents the potential energy along the z-axis, which is the tunneling direction and perpendicular to the Si/SiO_2 interface, E_z^s is the longitudinal energy of a tunneling electron in the substrate. It is noted that $\hbar^2k_r^2/2m^*_{\perp-\mathrm{Si}}$ is the transverse energy of a tunneling electron in the plane parallel to the Si/SiO_2 interface. According to the above equation, the difference of the effective electron mass between Si and SiO_2 can result in a change of the potential energy along the tunneling direction and affects the tunneling through the gate oxide.

The average tunneling electron energy can be written as $E=\frac{1}{2}m^*v^2+\frac{3}{2}k_BT_C$ (m^*, v, and T_C are the effective electron mass, electron velocity and electron temperature) [10]. The average tunneling electron thermal energy at the electron temperature T_C is $\frac{3}{2}k_BT_C$ when tunneling electrons are in equilibrium states (k_B is Boltzmann constant). Thus the potential energy along the tunneling direction in the oxide when the oxide voltage is zero can be obtained as:

$$\begin{aligned}\phi&=\phi_0-\frac{\hbar^2k_r^2}{2m^*_{\perp-\mathrm{Si}}}\left(1-\frac{m^*_{\perp-\mathrm{Si}}}{m^*_{ox}}\right)\\&=\phi_0-\left(\frac{1}{2}m^*_{\perp-\mathrm{Si}}(v_d)^2+\alpha k_BT\right)\left(1-\frac{m^*_{\perp-\mathrm{Si}}}{m^*_{ox}}\right)\end{aligned} \quad (2)$$

where T is the device temperature, ϕ_0 the barrier height, v_d drift velocity, α a parameter characterizing the relation between the electron temperature in the plane parallel to the Si/SiO_2 interface and the device temperature ($\alpha=T_C/T$). In this paper $\alpha=1$. Thus tunneling current can be calculated by using the following equation [15]:

$$J=\int_0^\infty\frac{qm^*_{z-\mathrm{Si}}k_BT}{2\pi^2\hbar^3}D(E_z)\ln\left(\frac{1+\exp(E_{f-L}-E_z)}{1+\exp(E_{f-R}-E_z-qV_{ox})}\right)dE_z \quad (3)$$

where $m^*_{z-\mathrm{Si}}$ is the effective electron mass in the silicon along the tunneling direction E_{f-L} and E_{f-R} are the Fermi levels of the left contact and the right contact, respectively. The transmission coefficient

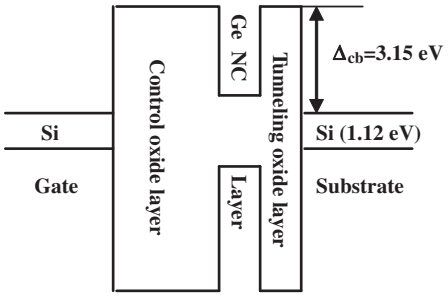

Fig. 1. Potential band structure of a Ge NC memory device.

can be calculated using transfer matrix method. The band structure of a Ge NC memory device used in the paper is shown in Fig. 1. Thus the tunneling current through the tunneling oxide layer and the total gate oxide including NC layer can be calculated. The transmission coefficient $D(E_z)$ can be calculated by a numerical solution of the one-dimensional Schrödinger equation. A parabolic $E(k)$ relation with an effective mass m^* has been assumed in this work. The barrier has been discretized by N partial subbarriers of rectangular shape that cover the whole gate oxide layer. From the continuity of wave-function and quantum current density at each boundary, the transmission coefficient through the gate oxide is then found by [15]:

$$D(E_z)=\frac{m_0}{m_{N+1}}\frac{k_{N+1}}{k_0}\frac{|\det M|}{|M_{22}|^2} \quad (4)$$

where M is a (2×2) product matrix, M_{22} is the quantity of the second row and the second column in this matrix $M=\prod_{l=0}^{N}M_l$ with transfer matrices M_l given by:

$$M_l=\frac{1}{2}\begin{vmatrix}(1+S_l)\exp[-i(k_{l+1}-k_l)x_l] & (1-S_l)\exp[-i(k_{l+1}+k_l)x_l]\\(1-S_l)\exp[+i(k_{l+1}-k_l)x_l] & (1+S_l)\exp[+i(k_{l+1}-k_l)x_l]\end{vmatrix} \quad (5)$$

In the above equation, $S_l=m_{l+1}k_l/m_lk_{l+1}$, and the effective masses and momenta has been discretized as $m_l=m^*[(x_{l-1}+x_l)/2]$ and $k_l=k[(x_{l-1}+x_l)/2]$, respectively, x_l is the position of lth boundary. The Fermi–Dirac distribution has been used in the tunneling current calculations of this work, and the maximum of the longitudinal electron energy (z-direction) was set at $20k_BT$ above the bottom of the conduction (valance) band.

The stored charge density for a Ge NC memory device can be calculated using:

$$\frac{dQ}{dt}=-J_{t-ox}+J_g \quad (6)$$

where J_{t-ox} and J_g are the tunneling current through the tunneling oxide layer and the total gate oxide including NC layer, respectively. In order to calculate the transmission coefficient, the electronic field across the gate oxide is needed. When the gate is applied a positive voltage and assume that the oxide voltage is V_{ox}, the electric field across the tunneling oxide layer can be deduced via solution to the Poisson's equation under the boundary conditions:

$$E_{t-ox}=\frac{V_{ox}+\frac{\sigma}{\varepsilon_2}d_2\left(\frac{\varepsilon_2}{\varepsilon_3}d_3+\frac{1}{2}d_2\right)}{\left(d_1+\frac{\varepsilon_1}{\varepsilon_3}d_3+\frac{\varepsilon_1}{\varepsilon_2}d_2\right)} \quad (7)$$

where d_1, d_2, and d_3 are the thickness of the tunneling oxide layer, Ge NC layer, and control oxide layer, respectively. ε_1, ε_2, and ε_3 are the dielectric constant of the tunneling oxide layer, Ge NC layer, and control oxide layer, respectively. σ is the linear density of the stored charge in the Ge NC Layer along the tunneling direction. Thus the shift in the threshold voltage can be written as:

$$\Delta V_{th}=\frac{\sigma}{\varepsilon_2}d_2\left(\frac{\varepsilon_2}{\varepsilon_3}d_3+\frac{1}{2}d_2\right) \quad (8)$$

The size-dependent dielectric constant of Ge NCs is given by [5]:

$$\varepsilon(d)=1+\frac{\varepsilon_b-1}{1+\left(\frac{d_0}{d/2}\right)^{1.1}} \quad (9)$$

where ε_b is the dielectric constant of bulk germanium. The characteristic radius d_0 for Ge is 3.5 nm [5]. In order to extract the dielectric constant pertaining to the nanocrystals, the simple superposition formula is:

$$\varepsilon = f\varepsilon(d) + (1-f)\varepsilon_b \tag{10}$$

where f is the filling factor that is the ratio of the area of Ge NCs to the total area. Note that the average density of Ge NCs according to the law [1,2].

$$D_{NC} \approx 6 \times 10^{-3}/d_2^2 \tag{11}$$

Also note that the Ge NCs have a truncated spherical form and present an aspect ratio (height over diameter) of about 0.8 [1,2]. Thus the filling factor that is the ratio of the area of Ge NCs to the total area can be obtained as:

$$f = \frac{6 \times 10^{-3}}{d_2^2} \times \pi \left(\frac{d}{2}\right)^2 = 0.2309 \tag{12}$$

In order to calculate the transmission coefficient, the barrier height for the gate oxide and the Ge NC layer are also needed. The energy of the highest valence state (E_v) and the energy of the lowest conduction state (E_c) for spherical NCs of diameter d (given in nanometer) are given by the following expression [4]:

$$E_c(d) = E_c(\infty) + \frac{11863.7}{d^2 + 2.391d + 4.252}\ (\text{meV}) \tag{13}$$

$$E_v(d) = E_v(\infty) - \frac{15143.8}{d^2 + 6.465d + 2.546}\ (\text{meV}) \tag{14}$$

When Ge NCs in the deposited amorphous Ge layer is charged with one elementary charge via tunneling, which causes a voltage buildup $V = Q/C_{nc\text{-}Ge}$, hence the amount of energy stored in this layer is:

$$E = Q^2/(2C_{nc\text{-}Ge}) \tag{15}$$

where Q is the charge density stored in the Ge NC layer, and $C_{nc\text{-}Ge}$ is the capacitance of the Ge NC layer.

3. Results and discussion

In this paper, the effective electron mass $0.5m_0$ of SiO_2, $0.26m_0$ of silicon, and $0.12m_0$ of Ge NC [16], the relative dielectric constant of the SiO_2, Si, and Ge of 3.9, 11.9, and 16 [17] have been used in this paper. The published electron affinities of crystalline silicon, SiO_2, and Ge are 4.05 eV, 0.9 eV, and 4.0 eV respectively [18]. For Si(100) surface, the effective mass of an electron along the direction perpendicular to plane and in the plane were chosen as $0.432m_0$ and $0.341m_0$ respectively according to Ref. [19]. In this article, for simplicity, $m_z^* = 0.26m_0$. In all calculations except the comparison between theory and experiment, the initial voltage across the total oxide containing Ge NC layer is 20 V, the size of Ge NC is 3.5 nm, and the thickness of the tunneling oxide layer and the control oxide layer are 2 nm and 25 nm, respectively.

In order to validate the theory, a comparison between theoretical data using the parameters in Ref. [17] and experimental data that come from Ref. [17] is given in Fig. 2. Good qualitative agreement is observed between theory and experiment in Fig. 2, although some quantitative disagreements still remain and need explanation. In the calculation of Fig. 2 (the following Figs. 3 and 4), the effect of the drift velocity of the channel electron on the stored charge in the Ge NC layer has been neglected. The deviance in quantity might origins from that the charge captured by defects in the oxide and the Ge NC layer, inappropriate data about effective electron mass for the oxide and the Ge NC layer and the barrier height between silicon substrate and ultrathin tunneling oxide layer, neglecting the drift velocity of the channel electron, and overestimate the dielectric constant of the Ge NC layer. One can note that both theoretical and experimental results obey the same tendency. According to Eq. (2), considering drift velocity and using it and the effective electron mass as fitting parameters, there can

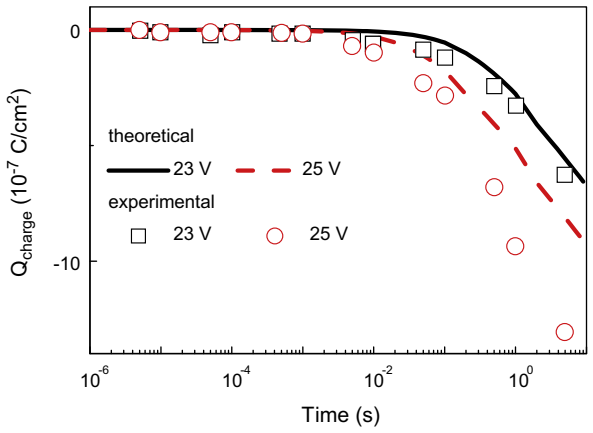

Fig. 2. Comparison of the stored charges as a function of the charging time between theory and experiment.

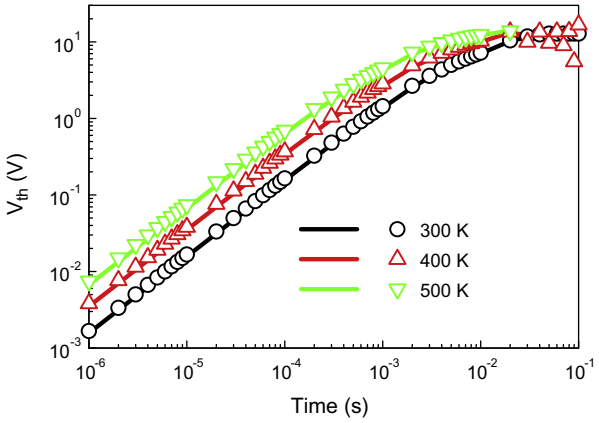

Fig. 3. Comparison of the threshold voltage as a function of the charging time between considering the quantum coupling effects and without. Symbols represent the results considering the quantum coupling effects. Lines represent the results neglecting the quantum coupling effects at different temperature with neglecting the effects of the drift velocity.

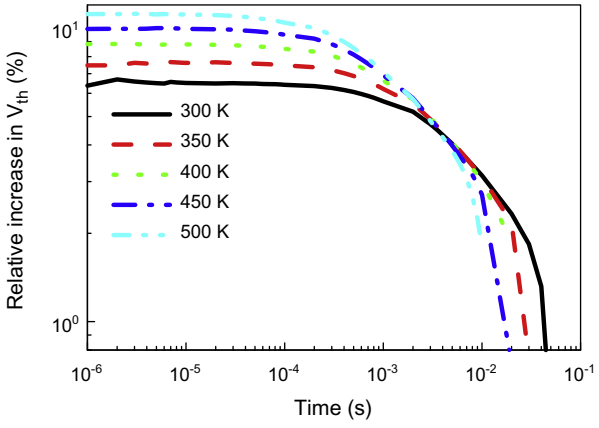

Fig. 4. The relative change in the threshold voltage calculated with considered the quantum coupling effects compared to those calculated without as a function of the charging time at different temperature with neglecting the effects of the drift velocity.

get a better fit for the case of 25 V because both have a large effect on the reduction in the barrier height and thus have a larger effect on the charging current. Such effects can be found in the following, see Figs. 5 and 8.

Fig. 3 shows that the threshold voltage changes with the charging time when the temperature is 300 K, 400 K, and 500 K, respectively. The threshold voltage is found to be an initial rapid increase, then saturation with the charging time for all temperature. Note that the electric field across the tunneling oxide layer decrease with the increasing electron density stored in the Ge NC layer according to Eq. (7). When the electron density stored in the Ge NC layer is large enough at a given gate voltage, the electric field across the tunneling oxide layer could be zero. Thus there need a balance between the charge and discharge, which leads to the fluctuations observed in Fig. 3.

Fig. 4 demonstrates that relative change in the threshold voltage calculated with considered the quantum coupling effect compared to those neglecting the quantum coupling effects changes with the charging time. The relative change in the threshold voltage considered the quantum coupling effects compared to those neglecting the quantum coupling effects is found to decrease with the charging time increasing. The reason is that the quantum coupling effects leads to a larger charging current, thus a more charge stored in the Ge NC layer for the same charging time, whereas a more charge stored in the Ge NC layer result in a decrease in the electric field across the tunneling oxide layer according to Eq. (7) and thus an exponential decrease in the tunneling probability and tunneling current, which implies a lower voltage drop across the tunneling oxide layer and a smaller charging current. The phenomenon about the charging current observed in Fig. 4 is a compromise between the quantum coupling effects on the tunneling current and the charge stored in the Ge NC layer on the electric field across the tunneling oxide layer. In the following, we discuss the difference between the threshold voltage calculated with and without the quantum coupling effects. According to Eq. (6) and

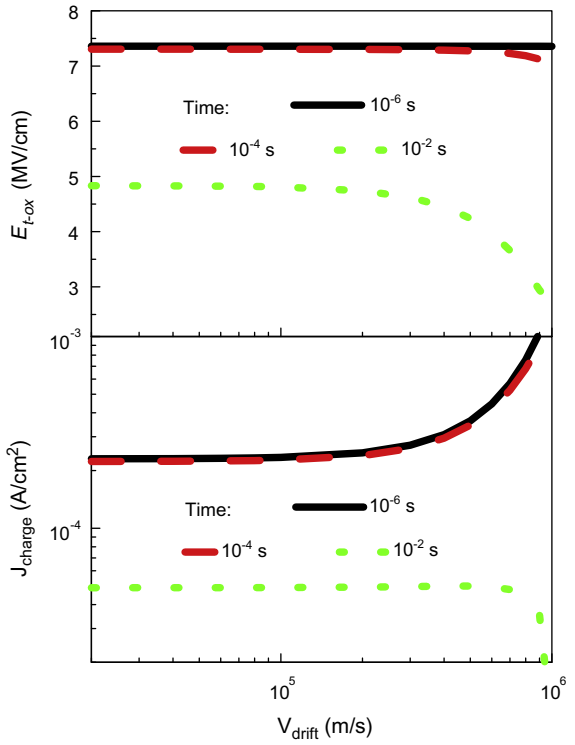

Fig. 5. The charging current and the electric field across the tunneling oxide layer as a function of the drift velocity due to the quantum coupling effects at temperature of 300 K for different charging time.

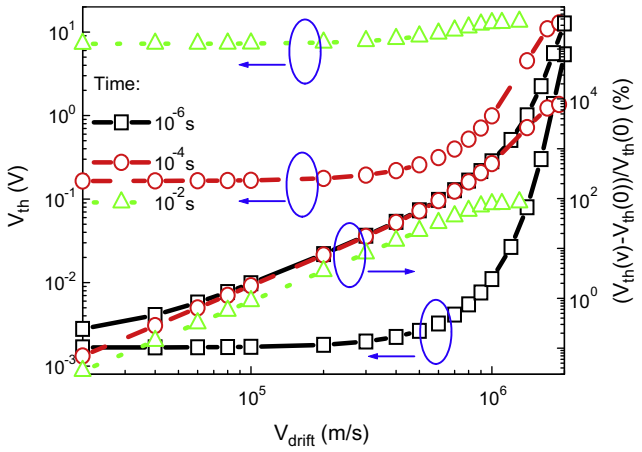

Fig. 6. The threshold voltage and its relative change calculated with considered the quantum coupling effects compared to those calculated without as a function of the drift velocity at temperature of 300 K for different charging time.

Eq. (8) with the assumption that $J_{t-ox} \gg J_g$, the variation of the threshold voltage can be obtained as $\Delta V_{th} = \frac{\int_0^t J_{t-ox}(t)\times dt}{\varepsilon_2}\left(\frac{\varepsilon_2}{\varepsilon_3}d_3 + \frac{1}{2}d_2\right)$. For Fowler–Nordheim tunneling current can be described as [20]: $J = AE_{ox}^2 \exp(-\frac{B}{E_{ox}})$ (here $A = \frac{q^3}{16\pi^2\hbar}\frac{m^*_{z-Si}}{m_{ox}\phi_B}$, $B = \frac{4}{3}\frac{(2m_{ox})^{1/2}}{q\hbar}(\phi_B)^{3/2}$, ϕ_B is the tunneling barrier height) and the direct tunneling current can be written as [21], $J_{DT} = \frac{A}{\alpha(E_{ox})}E_{ox}^2 \exp\left[-\frac{B}{E_{ox}}\beta(E_{ox})\right]$ (where $\alpha(E_{ox}) = \left[1 - (\frac{\phi_B - qt_{ox}E_{ox}}{\phi_B})^{1/2}\right]^2$, $\beta(E_{ox}) = \frac{\phi_B^{3/2} - (\phi_B - qt_{ox}E_{ox})^{3/2}}{\phi_B^{3/2}}$, t_{ox} is the oxide thickness, E_{ox} is the oxide field). For both tunneling, the reduction in the barrier height leads to a decrease in the quantity of B, and thus the tunneling current with considering the quantum coupling effects is larger than those without. On the other hand, the electric field across the tunneling oxide layer decrease with increasing electron density stored in the Ge NC layer according to Eq. (7), which also cause a large increase in the tunneling current from the above equations.

Fig. 5 depicts how the drift velocity under the consideration of the quantum coupling effects affects on the charging current and the electric field across the tunneling oxide layer. One can find that the charging current rapidly increase with the drift velocity for the initial stage especially on the drift velocity higher the thermal

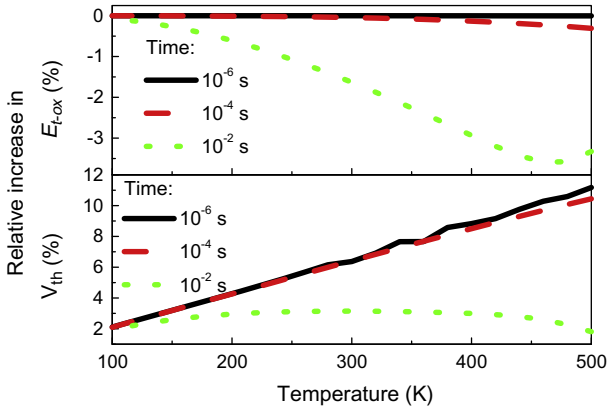

Fig. 7. The relative change in threshold voltage and the electric field across the tunneling oxide layer calculated with considered the quantum coupling effects compared to those calculated without as a function of temperature at different charging time with neglecting the effects of the drift velocity.

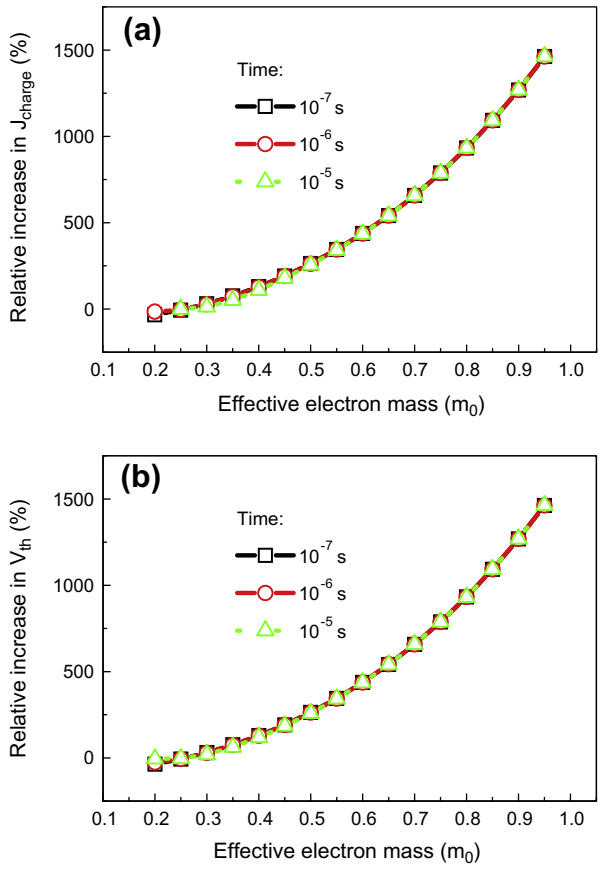

Fig. 8. The relative change in the charging current (a) and the threshold voltage (b) calculated with considered the quantum coupling effects compared to those calculated without as a function of the effective electron mass of SiO_2 at temperature of 300 K for different charging time with neglecting the effects of the drift velocity.

velocity. On the other hand, the electric field across the tunneling oxide layer decreases with increasing drift velocity especially on the drift velocity higher the thermal velocity.

Fig. 6 shows how the drift velocity under the consideration of the quantum coupling effects affects on the threshold voltage and its relative change. One can note that the threshold voltage rapidly increase with increasing drift velocity especially on the drift velocity higher the thermal velocity. It implies that the change in the threshold voltage caused by the channel electron velocity due to the effective electron mass difference between silicon and oxide can be neglected when the channel electron velocity is less than the thermal velocity.

Fig. 7 depicts the relative increase in the threshold voltage and the electric filed across the tunneling oxide calculated with considered the quantum coupling effects compared to those calculated without considering quantum coupling effects. The threshold voltage increases linearly with the temperature in the initial stage of the charging process. According to Eqs. (7) and (8), a more charge stored in the Ge NC layer will result in an increase in the threshold voltage and a decrease in the electric field across the tunneling oxide layer, which leads to a decrease in the tunneling current through the tunneling oxide layer. Whereas the reduction in the barrier height increasing with the temperature according to Eq. (2), which leads to an increase in the tunneling current through the tunneling oxide layer. The complicate relation between the relative change and the temperature in the later stage of the charging observed in this figure is a compromise between the above two factors.

Fig. 8a demonstrates that the relative change in the charging current calculated with considered the quantum coupling effects compared to those calculated without exponentially increases with increasing effective electron mass of the tunneling oxide layer. The temperature of 300 K has been used in the calculation with neglecting the effects of the drift velocity. One can note that the effective electron mass of the tunneling oxide have a large effect on the charging current due to the quantum coupling effect. It can be easily explained using Eq. (2). According to Eq. (2), the quantum coupling effects lead to an increase in the barrier height when the effective electron mass of the tunneling oxide layer decreases. Thus an increase the effective electron mass of the tunneling oxide leads to a decrease in the barrier height, and an increase in the transmission coefficient, and lastly leads to an increase in the charging current. It can be concluded from this figure that the charging current is strongly dependent on the effective electron mass of the tunneling oxide layer. Such a sensitivity of the effective electron mass of the tunneling oxide layer on the charging current can be proposed as a potential method to improve charging dynamics. Fig. 8b also shows similar trends for threshold voltage changing with the effective electron mass of the tunneling oxide layer at three given charging time. Strong sensitivity of the threshold voltage on the effective electron mass of the tunneling oxide layer can be also observed due to the above reason.

4. Conclusions

In conclusion, the quantum coupling effects on the charging dynamics of Ge NC memory devices for different temperature and drift velocity have been theoretically investigated. The relative change in the threshold voltage calculated with considered the quantum coupling effects compared to those calculated without is found to decrease with the charging time. It is caused by a compromise between the effects of an increase in the tunneling current due to the quantum coupling effects (Eqs. (2) and (3)) and a decrease in the electric field across the tunneling oxide layer with increasing charge density stored in the Ge NC layer (Eq. (7)). Theoretical analysis also demonstrates that the electric field across the tunneling oxide layer initially keep constant, then slowly decrease, and lastly rapidly decrease with the drift velocity and temperature due to the quantum coupling effects. It is worthy of being noted that the quantum coupling effects must be considered for high temperature and the drift velocity higher than the thermal velocity. The theoretical analysis (Eq. (2) and (3)) also demonstrates that the charging current strongly depends on the drift velocity, the temperature and the effective electron mass of the tunneling oxide layer. The calculations also demonstrate that the charging current and the threshold voltage at a given charging time shows such a strong sensitivity on the effective electron mass of the tunneling oxide layer. This sensitivity of the effective electron mass of the tunneling oxide layer on the charging current can be proposed as a potential method to improve charging dynamics.

Acknowledgments

The author acknowledges financial support from the National Natural Science Foundation of China under Grant 61076102 and Natural Science Foundation of Jiangsu Province under Grant BK2012614.

References

[1] Szkutnik PD, Karmous A, Bassani F, Ronda A, Berbezier I, Gacem K, et al. Ge nanocrystals formation on SiO_2 by dewetting: application to memory. Eur Phys J Appl Phys 2008;41:103–6.

[2] El Hdiy A, Gacem K, Troyon M, Ronda A, Bassani F, Berbezier I. Germanium nanocrystal density and size effects on carrier storage and emission. J Appl Phys 2008;104. 063716-1-3.
[3] Akca IB, Dâna A, Aydinli A, Turan Rt. Comparison of electron and hole charge-discharge dynamics in germanium nanocrystal flash memories. Appl Phys Lett 2008;92. 052103-1-3.
[4] Niquet YM, Allan G, Delerue C, Lannoo M. Quantum confinement in germanium nanocrystals. Appl Phys Lett 2000;77:1182–4.
[5] Weissker H-Ch, Furthmüller J, Bechstedt F. Optical properties of Ge and Si nanocrystallites from ab initio calculations. II. Hydrogenated nanocrystallites. Phys Rev B 2002;65. 155328-1-7.
[6] Gacem K, El Hdiy A, Troyon M, Berbezier I, Szkutnik PD, Karmous A, et al 2007;102. 093704-1-4.
[7] Yang M, Chen TP, Wong JI, Ng CY, Liu Y, Ding L, et al. J Appl Phys 2007;101. 124313-1-5.
[8] Mao LF. Dot size effects of nanocrystalline germanium on charging dynamics of memory devices. Nanoscale Res Lett 2013;8. 21-1-4.
[9] Mao LF. Interface traps and quantum size effects on the retention time in nanoscale memory devices. Nanoscale Res Lett 2013;8. 369-1-5.
[10] Mao LF. Temperature dependence of the tunneling current in metal-oxide-semiconductor devices due to the coupling between the longitudinal and transverse components of the electron thermal energy. Appl Phys Lett 2007;90:183511.
[11] Mao LF. The effects of the injection-channel velocity on the gate leakage current of nanoscale MOSFETs. IEEE Electron Dev Lett 2007;28:161–3.
[12] Mao LF. Modeling of temperature dependence of the leakage current through hafnium silicate gate dielectric in a MOS device. Semicond Sci Technol 2007;22:1203–8.
[13] Mao LF. The effects of the in-plane momentum on the quantization of nanometer metal-oxide-semiconductor devices due to the difference between the effective masses of silicon and gate oxide. Appl. Phys. Lett. 2007;91. 123519-1-3.
[14] Mao LF. Effects of in-plane momentum of channel electron on the capacitance–voltage curve in n-MOS devices. ETRI J 2010;32:68–74.
[15] Ando Y, Itoh T. Calculation of transmission tunneling current across arbitrary potential barriers. J Appl Phys 1987;61:1497–502.
[16] Adikaari AADT, Carey JD, Stolojan V, Keddie JL, Silva SRP. Bandgap enhancement of layered nanocrystalline silicon from excimer laser crystallization. Nanotechnology 2006;17:5412–6.
[17] Yue G-Z, Kong G-L, Zhang D-L, Ma Z-X, Sheng S-R, Liao X-B. Dielectric response and its light-induced change in undoped a-Si:H films below 13 MHz. Phys Rev B 1998;57:2387–92.
[18] Matsuura H, Okuno T, Okushi H, Tanaka K. Electrical properties of n-amorphous/p-crystalline silicon heterojunctions. J Appl Phys 1984;55:1012–9.
[19] Vexler MI, Tyaginov SE, Shulekin AF. Determination of the hole effective mass in thin silicon dioxide film by means of an analysis of characteristics of a MOS tunnel emitter transisto. J Phys: Condens Matter 2005;17:8057–68.
[20] Depas M, Vermeire B, Mertens PW, Van Meirhaeghe RL, Heyns MM. Determination of tunnelling parameters in ultra-thin oxide layer poly-Si/SiO_2/Si structures. Solid-State Electron 1995;38:1465–71.
[21] Wei JL, Mao LF, Xu M, Tan C. Direct tunneling relaxation spectroscopy in ultra-thin gate oxide MOS structures. Solid-State Electron 2000;44:2021–5.